

## Bimetallic Ni-Co/Al<sub>2</sub>O<sub>3</sub> Catalysts Derived from Aluminate Spinels for Dry Reforming of Methane

Andoni Choya\*, Julen Ibañez, Beatriz de Rivas, Jose I. Gutiérrez-Ortiz, Rubén López-Fonseca

Chemical Technologies for Environmental Sustainability Group, Department of Chemical Engineering, Faculty of Science and Technology, University of the Basque Country/EHU, PO Box 644, E-48080 Bilbao, Spain  
 andoni.choya@ehu.eus

Five Ni-Co/Al<sub>2</sub>O<sub>3</sub> catalysts for dry reforming of methane were obtained by high-temperature reduction of mixed Ni-Co spinel aluminates (Ni<sub>x</sub>Co<sub>1-x</sub>Al<sub>2</sub>O<sub>4</sub>) synthesised by a precipitation route. The aim of the study was to determine the effect of the incorporation of cobalt to the nickel aluminate spinel to the activity and selectivity of the resulting catalysts. The results indicated that the addition of cobalt was generally detrimental for the textural and structural properties of the mixed catalysts with respect to the monometallic nickel counterpart, thus producing catalysts with lower metallic dispersion. However, the presence of cobalt in the reduced catalysts resulted in an enhanced selectivity towards H<sub>2</sub> generation. In addition to that, the lower Ni content of the mixed catalysts resulted in an improvement in stability. As a result, the Ni<sub>0.5</sub>Co<sub>0.5</sub>Al<sub>2</sub>O<sub>4</sub> mixed spinel was able to produce a Ni-Co/Al<sub>2</sub>O<sub>3</sub> catalyst that exhibited higher reactant conversions, H<sub>2</sub>/CO molar ratio of the product stream and higher stability than the Ni/Al<sub>2</sub>O<sub>3</sub> monometallic catalyst.

### 1. Introduction

The dry reforming of methane (DRM) reaction is process of a high environmental interest, since it converts CO<sub>2</sub> and CH<sub>4</sub> into syngas (H<sub>2</sub> + CO) with a H<sub>2</sub>/CO ratio of around 1 (Lavoie, 2014). Thus, DRM utilizes greenhouse gases, to produce an industrially important synthesis gas, which can be used for the manufacture of useful value-added products (Sternberg et al., 2017).

For this process, Ni-based catalysts are the most attractive and promising candidates instead of noble metals (Aramouni et al., 2018), since the nickel-support interaction created during the catalyst preparation allows it to overcome the main deactivation issues of these types of catalysts, which are coke formation and sintering. The source of coke during the DRM reaction can be attributed to two reactions, namely methane cracking and Boudouard reaction (Arora and Prasad, 2016). Simultaneously, the high temperatures (in the 650-900 °C range) required for the reaction generally causes an uncontrollable growth of the metallic particles (Kawi et al., 2015). An innovative approach for Ni catalyst synthesis is to introduce the transition metal into the structure of a crystalline precursor oxide such as the nickel aluminate spinel NiAl<sub>2</sub>O<sub>4</sub> (López-Fonseca et al., 2012). However, due to the stoichiometric requirements to completely form the NiAl<sub>2</sub>O<sub>4</sub> spinel, these catalysts normally present high Ni loadings (>30%wt.Ni), which make them prone to coking, especially at lower temperatures (Liu et al., 2011). The use of sub-stoichiometric Ni/Al spinel precursors has been found to produce catalysts that are more resistant to coking, although they tend to produce a syngas with a low H<sub>2</sub>/CO molar ratio, since highly dispersed nickel is also active for the reverse water gas shift (RWGS) reaction, which consumes H<sub>2</sub> and produces CO (Gil-Calvo et al., 2017).

In order to improve the H<sub>2</sub> selectivity of the process, a possible alternative would be the incorporation of a secondary metal that can inhibit the overall activity towards the RWGS reaction and activate other H<sub>2</sub> producing reactions, such as methane cracking. Following this approach, in this work, the addition of cobalt to the nickel spinel precursor is explored. The aim of the study is to obtain Ni-Co-Al mixed spinels that, after a proper activation, can result in active and stable catalysts that can also produce H<sub>2</sub>-enriched syngas with respect to the monometallic nickel counterpart.

## 2. Experimental methodology

To achieve the objective of this work, the following experimental methodology was followed:

### 2.1 Synthesis methodology

The monometallic and bimetallic spinel precursors were synthesized by the precipitation route, starting from nickel, cobalt and alumina nitrates and using sodium carbonate as the precipitating agent. Firstly, a solution of adjusted concentrations of the metallic nitrates was prepared and heated up to 80 °C, after which a solution of Na<sub>2</sub>CO<sub>3</sub> 1.2 M was added until pH reached 9. After an ageing period of 30 min, the precipitated solids were filtered and washed with 4 L of deionized water. The filtered solids were then dried at 110 °C overnight and the subjected to calcination at 850 °C for 4 hours under static air. The catalytic precursors were identified by their x value, where x represented the Ni/(Ni + Co) molar ratio, thus the general formula of the spinel precursors were Ni<sub>x</sub>Co<sub>1-x</sub>Al<sub>2</sub>O<sub>4</sub>. The chosen x values were 0, 0.25, 0.5, 0.75 and 1. All catalytic precursors were subjected to a reduction process with 5% H<sub>2</sub>/N<sub>2</sub> at 850 °C for 2 hours prior to the reaction experiments.

### 2.2 Characterisation techniques

The N<sub>2</sub> adsorption/desorption isotherms of the synthesised precursors and reduced catalysts were obtained with a Micromeritics Tristar II apparatus at 77 K. Prior to the analysis, each sample was subjected to degassing at 300 °C for 10 h in a Micromeritics SmartPrep degasser. The specific surface area of the samples was calculated from the adsorption isotherm using the BET method. X-ray diffraction experiments were carried out on an X'PERT-PRO X-ray diffractometer equipped with a Cu K $\alpha$  ( $\lambda$  = 1.5406 Å) X-ray source that was operated at 40 kV and 40 mA and a Ni filter. The diffractograms were taken between the 2 $\theta$  positions of 5 and 80° with a step size of 0.026°. The reducibility of the catalytic precursors was investigated on a Micromeritics Autochem 2920 apparatus by temperature-programmed reduction with hydrogen. Prior to the experiments, the samples were pre-treated with a 5% O<sub>2</sub>/He stream at 300 °C for 1 hour to completely oxidize them. Then, the experiments were carried out using a 5% H<sub>2</sub>/Ar mixture as the reducing agent from ambient temperature to 900 °C, after which a 30 min isotherm at 900 °C followed. The water generated during the process was removed from the stream before the TCD to avoid interference by passing it through a cold trap which was maintained at -90 °C with an isopropanol sludge cooled down with liquid nitrogen.

### 2.3 Reaction conditions

The activity of the reduced catalysts was assessed in a PID Eng&Tech Microactivity Reference bench-scale fixed bed tubular reactor. In each experiment, 0.1 g of catalyst (0.25– 0.3 mm particles) were diluted with 0.9 g of quartz (0.5–0.8 mm particles) and placed inside a quartz glass tube with a type-K thermocouple placed inside to control the temperature of the catalytic bed. The activity experiments were performed at constant temperature of 650 °C for 12 hours by feeding a gaseous mixture of 10%CH<sub>4</sub>/10%CO<sub>2</sub>/80%N<sub>2</sub> at 1.2 L min<sup>-1</sup>. Under these conditions, the GHSV was around 90,000 h<sup>-1</sup>. The composition of the outlet stream from the reactor was monitored by a microGC equipped with two separation columns, each coupled to a TCD.

## 3. Results and Discussion

Below, the main results from the characterisation and catalytic testing of the samples are discussed.

### 3.1 Characterisation of the calcined precursors

The calcined spinel precursors were examined by N<sub>2</sub> physisorption, XRD and H<sub>2</sub>-TPR. The textural characterisation by N<sub>2</sub> physisorption evidenced that all calcined precursors were mesoporous materials (type IV isotherms) with relatively narrow pore size distributions (type H2 hysteresis cycle). The specific surface area of the precursors (Table 1) varied between 27 m<sup>2</sup> g<sup>-1</sup> for the CoAl<sub>2</sub>O<sub>4</sub> precursor (x = 0) and 82 m<sup>2</sup> g<sup>-1</sup> for the NiAl<sub>2</sub>O<sub>4</sub> spinel (x = 1). Thus, it was evident that the incorporation of cobalt to the nickel aluminate spinel did not have a positive effect over the textural properties of the resulting spinel.

Table 1: Physico-chemical properties of the calcined precursors

Sample	Specific surface area, m <sup>2</sup> g <sup>-1</sup>	Spinel phase crystallite size, nm	Relative abundance of spinelic phases, %
x = 0	27	45	81
x = 0.25	41	38	80
x = 0.50	52	20	79
x = 0.75	62	13	75
x = 1	82	9	72

The structural characterisation by XRD revealed the presence of a spinel cubic phase in all the calcined precursors with diffraction signals at  $2\theta = 19.1, 31.4, 37.0, 45.0, 55.8, 59.6$  and  $65.5^\circ$ , which could be attributed to the presence of  $\text{CoAl}_2\text{O}_4$  (ICDD 044-0160) and/or  $\text{NiAl}_2\text{O}_4$  (ICDD 010-0339). Also, for the samples with  $x$  higher than 0.25, additional signals at  $2\theta = 43.3$  and  $62.9^\circ$  appeared, which were associated with the presence of segregated  $\text{NiO}$  (ICDD 047-1049). In addition to that, a close-up view of the most intense signal of the spinel phase at  $2\theta = 37.0^\circ$  (Figure 1) evidenced a shift towards higher positions with the increase of the  $x$  value, which indicated a shrinkage of the cell parameter of the spinel. This would be in agreement with the smaller cell parameter of  $\text{NiAl}_2\text{O}_4$  (8.048 Å) with respect to  $\text{CoAl}_2\text{O}_4$  (8.104 Å). The crystallite size of the spinel phase, estimated by the Scherrer equation from the most intense signal, varied from 45 nm for the  $\text{CoAl}_2\text{O}_4$  precursor to 9 nm for the  $\text{NiAl}_2\text{O}_4$  counterpart, in line with the previous values for the specific surface area.

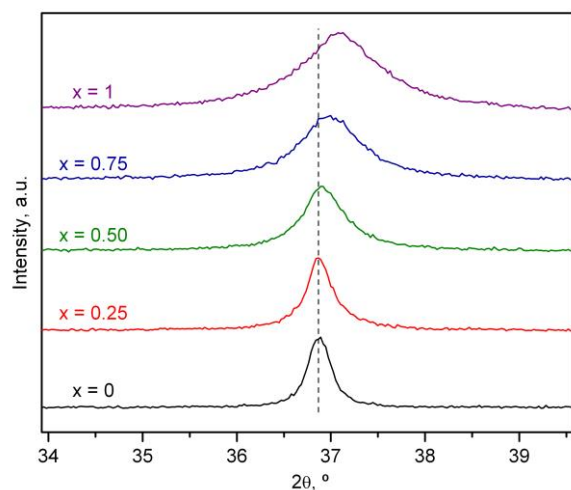


Figure 1: Close-up view of the XRD profiles of the calcined precursors in the 34-39° range.

The  $\text{H}_2$ -TPR profiles of the calcined precursors are included in Figure 2. All reduction traces were characterised by a two-step process in which the first step, located between 350 and 650 °C corresponded to the reduction of segregated metallic oxides, namely  $\text{NiO}$  and small amounts of  $\text{Co}_3\text{O}_4$  (Lim et al., 2015), while the second step, centred around 850 °C, was attributed to the reduction of the aluminate spinels (Garbarino et al., 2015). The integration and quantification of the reduction traces allowed for the calculation of the  $\text{H}_2$  uptake for each step that served to estimate the relative abundance of spinel phase present in each precursor, as presented in Table 1. The results pointed out that the calcined oxide precursors contained between 72 and 81% of aluminate phases, with the percentage being higher for the lower values of the parameter  $x$ , thus suggesting that  $\text{CoAl}_2\text{O}_4$  forms slightly more efficiently than  $\text{NiAl}_2\text{O}_4$ .

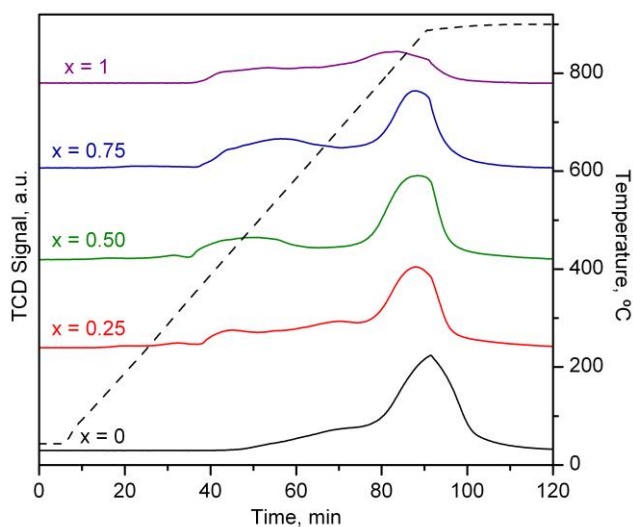


Figure 2:  $\text{H}_2$ -TPR profiles of the calcined spinel precursors.

### 3.2 Characterisation of the reduced catalysts

The textural characterisation of the reduced Ni-Co catalysts evidenced that the reduction process did not significantly affect the pore structure of the samples since all presented the same aforementioned type IV isotherms with H2 hysteresis cycles. However, the reduction process entailed a loss of specific surface area of around 30% with respect to the calcined precursors, as shown in the results presented in Table 2. Thus, the reduced catalysts exhibited specific surface areas between  $20 \text{ m}^2 \text{ g}^{-1}$  ( $x = 0$ ) and  $57 \text{ m}^2 \text{ g}^{-1}$  ( $x = 1$ ).

Table 2: Physico-chemical properties of the reduced catalysts

Sample	Specific surface area, $\text{m}^2 \text{ g}^{-1}$	Metal crystallite size, nm
$x = 0$	20	23
$x = 0.25$	29	22
$x = 0.50$	36	17
$x = 0.75$	43	15
$x = 1$	57	13

The XRD patterns of the reduced catalysts (Figure 3) presented signals of cubic phase metallic crystallites at  $2\theta = 44.4$ ,  $51.8$  and  $76.1^\circ$ , which could be attributed the metallic Ni (ICDD 004-0850) and Co (ICDD 015-0806) crystallites formed in the reduction of the spinel precursors. In addition, signals located at  $2\theta = 37.7$ ,  $45.9$  and  $66.9^\circ$  pointed to the presence of  $\gamma\text{-Al}_2\text{O}_3$  (ICDD 01-074-2206) also formed during the reduction of the spinel precursors.

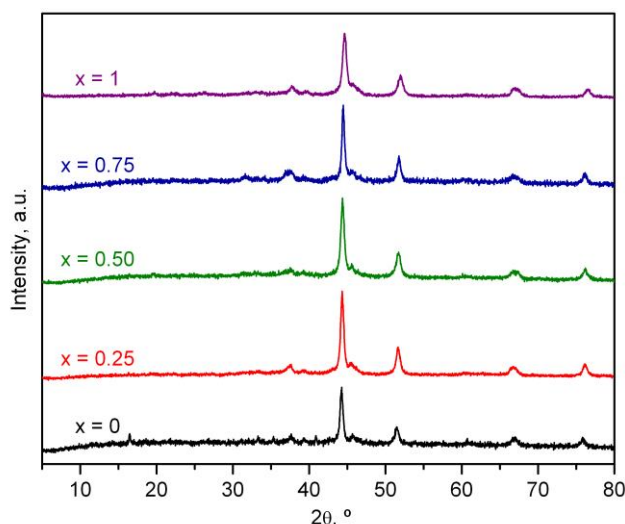


Figure 3: XRD profiles of the reduced Ni-Co catalysts.

The average crystallite size of the metallic Ni and Co, shown in Table 2, varied between 23 nm ( $x = 0$ ) and 13 nm ( $x = 1$ ). It must be noticed that it was not possible to determine the individual sizes of the Ni and Co crystallites due to their respective diffraction signals being too similar. Thus, the aforementioned values could be taken as an average of the crystallite size of both metallic species. In any case, the results indicated that metallic dispersion improved with the nickel content of the catalysts.

### 3.3 Catalytic activity of the reduced catalysts

The efficiency of the reduced Ni-Co/ $\text{Al}_2\text{O}_3$  catalysts for the dry reforming of methane reaction was evaluated at constant temperature ( $650^\circ\text{C}$ ) for 12 hours at  $90,000 \text{ h}^{-1}$ . The behaviour of the catalysts along this reaction interval was evaluated by analysing the evolution of the  $\text{CH}_4$  conversion with time on stream, as presented in Figure 4. Among the studied samples, those with  $x = 0.50$  and  $x = 1$  achieved the highest initial conversion values (80 and 71%, respectively). However, the catalyst with  $x = 1$  ( $\text{NiAl}_2\text{O}_4$ ) suffered a notable deactivation after only 6 hours of reaction time and its conversion levels started decreasing, reaching 63% by the end of the experiment, while the rest of the catalysts were able to maintain a stable conversion throughout the duration of

the reaction test. Hence, the results pointed out that the addition of cobalt increased the stability of the nickel catalysts.

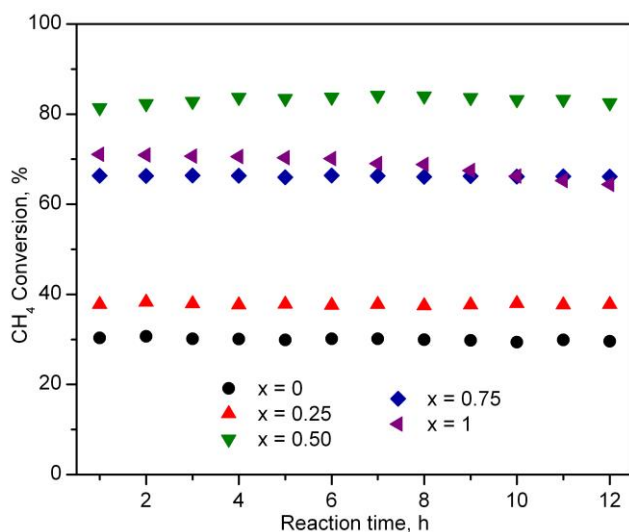


Figure 4: Evolution of the CH<sub>4</sub> conversion of the reduced catalysts with time on stream.

Moreover, the analysis of the relationship between the cobalt content of the Ni-Co catalysts and the H<sub>2</sub>/CO molar ratio of the product stream after 12 hours (Figure 5) evidenced that the presence of cobalt promoted the generation of H<sub>2</sub> in the dry reforming reaction. Thus, the H<sub>2</sub>/CO molar ratio increased from 0.85 for the NiAl<sub>2</sub>O<sub>4</sub>-derived catalyst up to 1.32 for the CoAl<sub>2</sub>O<sub>4</sub> counterpart despite the latter achieving significantly lower reactant conversions than the former.

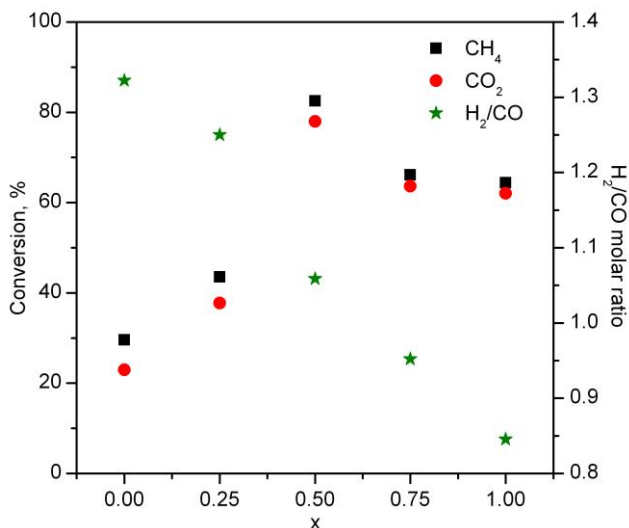


Figure 5: Relationship between the reaction parameters after 12 hours and x value of the reduced catalysts.

This behaviour was probably owing to the fact that cobalt was significantly less active than nickel for the reverse water gas shift reaction that consumes H<sub>2</sub> (Ranjbar et al., 2018), while at the same time being more active for the methane cracking reaction that generates it (Horlyck et al., 2018). Thus, despite being less active for the dry reforming reaction, the addition of a certain amount of cobalt to the nickel catalyst enhances the generation of H<sub>2</sub>. From the correlation described in Figure 5, it is clear that a Ni/Co molar ratio of 1 (x = 0.50) is the optimal formulation for the Ni-Co bimetallic catalyst due to combining a good metallic dispersion (small crystallite size with moderate specific surface areas), with an equilibrated Ni and Co loading. This led to a marked activity for

the dry reforming reaction with a limited selectivity for the reactions that inherently lower the H<sub>2</sub>/CO molar ratio, thus achieving high reactant conversions and a notable H<sub>2</sub> generation at the same time.

#### 4. Conclusions

Various bimetallic Ni-Co/Al<sub>2</sub>O<sub>3</sub> catalysts derived from spinel-like aluminates were synthesised for the dry reforming of methane reaction, with the aim of evaluating the effect of incorporating cobalt in different proportions to nickel. The characterisation of the aluminate precursors pointed out that the addition of cobalt decreased the specific surface area of the resulting catalysts (from 57 to 20 m<sup>2</sup> g<sup>-1</sup>) and increased the average crystallite size (from 13 to 23 nm), thus it was detrimental for the textural and structural properties of the resulting precursors and catalysts. In line with this, the catalytic activity results evidenced that the presence of cobalt in the bimetallic catalysts decreases their overall activity, with methane conversions being as low as 25% for the monometallic cobalt catalyst while the Ni counterpart achieved 70%. However, the results also pointed out that the presence of cobalt greatly enhanced the generation of H<sub>2</sub>. Thus, an optimal formulation of Ni<sub>0.5</sub>Co<sub>0.5</sub>Al<sub>2</sub>O<sub>4</sub> was identified that presented a higher activity (28% more CH<sub>4</sub> conversion) and a 50% more H<sub>2</sub> yield with respect to the Ni monometallic one.

#### Acknowledgments

This research was funded by the Spanish Ministry of Science and Innovation (PID2019-107105RB-I00 AEI/FEDER, UE), Basque Government (IT1509-22) and the University of The Basque Country UPV/EHU (DOCREC21/23). The authors wish to thank the technical and human support provided by SGIker (UPV/EHU).

#### References

- Aramouni N.A.K., Touma J.G., Tarboush B.A., Zeaiter J., Ahmad M.N., 2018, Catalyst Design for Dry Reforming of Methane: Analysis Review, *Renewable and Sustainable Energy Reviews* 82, 2570-2585.
- Arora S., Prasad R., 2016, An Overview on Dry Reforming of Methane: Strategies to Reduce Carbonaceous Deactivation of Catalysts, *RSC Advances* 6, 108668-108688.
- Garbarino G., Chitsazan S., Phung T.K., Riani P., Busca G., 2015, Preparation of Supported Catalysts: A Study of the Effect of Small Amounts of Silica on Ni/Al<sub>2</sub>O<sub>3</sub> Catalysts, *Applied Catalysis A: General*, 505, 86–97.
- Gil-Calvo M., Jiménez-González C., de Rivas B., Gutiérrez-Ortiz J.I., López-Fonseca R., 2017, Effect of Ni/Al Molar Ratio on the Performance of Substoichiometric NiAl<sub>2</sub>O<sub>4</sub> Spinel- Based Catalysts for Partial Oxidation of Methane, *Applied Catalysis B: Environmental*, 209, 128-138.
- Horlyck J., Lawrey C., Lovell E.C., Amal R., Scott J., 2018, Elucidating the Impact of Ni and Co Loading on the Selectivity of Bimetallic NiCo Catalysts for Dry Reforming of Methane, *Chemical Engineering Journal*, 352, 572-580.
- Kawi S., Kathiraser Y., Ni J., Oemar U., Li Z., Saw E.T., 2015, Progress in Synthesis of Highly Active and Stable Nickel-Based Catalysts for Carbon Dioxide Reforming of Methane, *ChemCatChem* 8, 3556-3575.
- Lavoie J-M., 2014, Review on Dry Reforming of Methane, a Potentially more Environmentally-Friendly Approach to the Increasing Natural Gas Exploitation, *Frontiers in Chemistry*, 2, Article 81.
- Lim T.H., Cho S.J., Yang H.S., Engelhard M.H., Kim D.H., 2015, Effect of Co/Ni Ratios in Cobalt Nickel Mixed Oxide Catalysts on Methane Combustion, *Applied Catalysis A: General*, 505, 62-69.
- Liu C-J., Ye J., Jiang J., Pan Y., 2011, Progresses in the Preparation of Coke Resistant Ni-based Catalyst for Steam and CO<sub>2</sub> Reforming of Methane, *ChemCatChem*, 3, 529-541.
- López-Fonseca R., Jiménez-González C., de Rivas B., Gutiérrez-Ortiz J.I., 2012, Partial Oxidation of Methane to Syngas on Bulk NiAl<sub>2</sub>O<sub>4</sub> Catalyst. Comparison with Alumina Supported Nickel, Platinum and Rhodium Catalysts, *Applied Catalysis A: General*, 437-438, 53-62.
- Ranjbar A., Irankhah A., Aghamiri S.F., 2018, Reverse Water Gas Shift Reaction and CO<sub>2</sub> Mitigation: Nanocrystalline MgO as a Support for Nickel Based Catalysts, *Journal of Environmental Chemical Engineering*, 6, 4945-4952.
- Sternberg A., Jens C.M., Bardow A., 2017, Life Cycle Assessment of CO<sub>2</sub>-based C1-Chemicals, *Green Chemistry* 19, 2244-2259.